

# A compact tunable 60-dB Faraday optical isolator for the near infrared

R. Wynands

*Max-Planck-Institut für Quantenoptik, Ludwig-Prandtl-Strasse 10, W-8046 Garching, Germany*

F. Diedrich

*Gsänger Optoelektronik GmbH, Robert-Koch-Strasse 1a, W-8033 Planegg 1, Germany*

D. Meschede

*Institut für Quantenoptik, Universität Hannover, Am Welfengarten 1, W-3000 Hannover, Germany*

H. R. Telle

*Physikalisch-Technische Bundesanstalt Braunschweig, Bundesallee 100, W-3300 Braunschweig, Germany*

(Received 15 July 1992; accepted for publication 14 August 1992)

We describe the concept and performance of a new type of tunable Faraday optical isolator for the near infrared. 60-dB isolation is achieved with three dielectric polarizers having an extinction of only 40 dB. The compact instrument does not cause an overall polarization rotation or beam displacement and gives access to all optical beams.

## I. INTRODUCTION

Diode lasers are becoming increasingly popular for precision applications such as communication systems, spectroscopy, frequency synthesis, and interferometry because they are relatively inexpensive, small, and easy to use.

However, a major drawback is their extreme sensitivity to optical feedback which can cause intensity instabilities, frequency pulling, and other unwanted effects. Thus it is usually necessary to isolate the diode laser by attenuating reflected and backscattered light by several orders of magnitude. In many cases, this can only be achieved with a Faraday optical isolator, as first proposed by Lord Rayleigh.<sup>1</sup> The fundamental arrangement (Fig. 1) consists of a linear polarizer, a "Faraday crystal" in a longitudinal magnetic field, and a second polarizer which is rotated by 45° with respect to the first one.

Light entering through the input polarizer experiences a rotation of its polarization direction. The angle of rotation,  $\alpha$ , is determined by

$$\alpha = V \int B(z) dz,$$

where  $V$  is the Verdet constant of the Faraday material in  $\text{rad}/(\text{T m})$ ,  $B$  is the magnetic flux density,  $z$  is the coordinate along the propagation direction of the light, and the integration is taken over the length of the crystal. With a proper choice of components  $\alpha$  can be made to be 45°. The light emerging from the crystal passes through the output polarizer without being attenuated. A light beam entering from the reverse direction is polarized by the output polarizer. In the crystal the polarization direction is subsequently rotated by 45°, but due to the nonreciprocity of the Faraday effect this rotation is in the same direction as before. With respect to the input polarizer the polarization of the backward traveling beam has been rotated by 90° in total, so no light can pass the input polarizer to get back into the laser.

An important characteristic of a Faraday isolator is that it extinguishes backscattered light independently of its

polarization direction. Very high isolation ratios are also possible. Here we define the isolation ratio as

$$E = -10 \log(I_r/I_0) \text{ dB},$$

where  $I_0$  is the light intensity incident on the isolator coming from the "wrong" (backward) direction and  $I_r$  is the intensity transmitted through the isolator towards the laser.

A useful diode laser isolator should meet the following specifications: 60-dB isolation ratio; continuous tunability over a wide range including 700–900 nm; 5-mm useful aperture; insertion loss below 1 dB; minimum wavefront distortion; no net polarization rotation; no beam displacement, even while tuning; all optical surfaces antireflection coated and slightly tilted against the beam axis to avoid direct reflection; all beams rejected at the polarizers should be available; the possibility of access to all outer surfaces for easy cleaning; convenient mounting in round or plane mounts; and smallest possible overall size and cost.

In the next section we will discuss the general concept of our isolator. Section III describes the individual components in detail, and the last sections discuss the performance of the isolator.

## II. ISOLATOR CONCEPT

To minimize the beam distortion by the crystal we used a single-pass design as opposed to the multipass geometries employed in some commercial devices. This also allows a larger useful aperture and makes alignment of the input beam less critical.

Due to residual double refraction in the Faraday material, it is very difficult (and expensive) to achieve more than 40 dB of isolation ratio with a single crystal. To obtain the desired 60-dB ratio we cascaded two traditional Faraday isolators with magnets of antiparallel magnetization (Fig. 2). This not only yields more than 60-dB isolation ratio but also offers the following practical advantages: (1) The net polarization rotation is zero. (2) Variation of the magnet separation allows coarse wavelength tuning since the stray field of one stage adds linearly to the axial

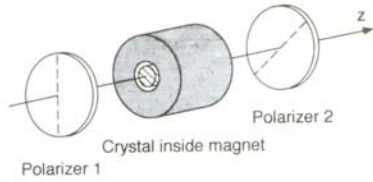


FIG. 1. General principle of the Faraday isolator.

field of the other one, increasing the total magnetic field at the crystals.<sup>2</sup> (3) Only one central polarizer is required. Moreover, rotating the polarization axis of this polarizer provides a way to fine tune the isolator at the expense of a small decrease in transmitted intensity. (4) The external stray field has a quadrupole rather than dipole characteristic with a more rapid drop off with distance. We will elaborate on these points in detail in the next section.

### III. COMPONENTS

#### A. Crystals

Terbium-gallium-garnet<sup>3</sup> (TGG) is currently the material of choice for near-infrared wavelengths because of its high Verdet constant. It offers  $V=60\text{--}110$  rad/(T m), a low absorption coefficient of  $\gamma=0.0015$  cm<sup>-1</sup>, and a thermal conductivity of  $\kappa=7.4$  W/(K m). A good terbium-doped glass is M-32 with  $V=45\text{--}80$  rad/(T m),  $\gamma=0.001$  cm<sup>-1</sup>, and  $\kappa=1$  W/(K m). Since the Verdet constant is temperature dependent, absorption in the crystal will lead to inhomogeneous Faraday rotation over the cross section of the beam. Therefore a material with a low absorption coefficient and high thermal conductivity is preferable.

For the isolator we chose TGG crystals 20 mm in length and 5 mm in diameter. To eliminate direct reflections the crystals have parallel faces tilted by 1° against the optic axis. The crystals of the two isolator stages are aligned such that the parallel beam displacement of both stages cancels, as indicated in the top of Fig. 3. Antireflection coatings on the facets help decrease the transmission losses. The crystals themselves are centered inside the magnets with a stress-free mount in order to avoid stress-induced birefringence.

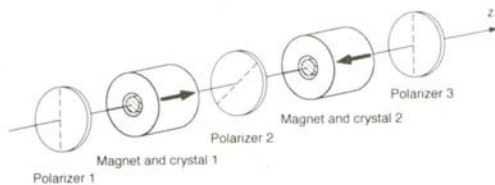


FIG. 2. Sketch of the geometrical arrangement of the two-stage Faraday isolator. Antiparallel magnetization of the magnets of the two stages has many advantages, as described in the text.

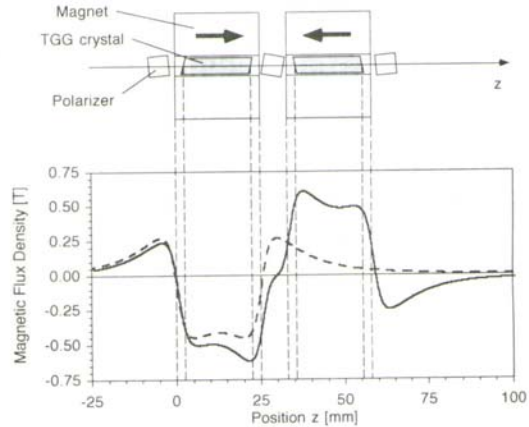


FIG. 3. Calculated magnetic flux density along the z axis. Dashed line: one magnet only; solid line: two magnets with antiparallel magnetization.

#### B. Magnets

We have chosen cylindrical magnets with axial magnetization and a cylindrical bore whose dimensions were optimized for maximum Faraday rotation at minimal volume. From elementary magnetostatics one can derive the flux density on the axis of a combination of two cylindrical permanent magnets of length  $2L$  and diameter  $2R$  with a central hole of diameter  $2r$  and opposite poling:

$$\begin{aligned}
 B(z) &= \frac{B_0}{2} \left( \frac{z+L}{\sqrt{(z+L)^2+R^2}} - \frac{z-L}{\sqrt{(z-L)^2+R^2}} \right) \\
 &\quad - \frac{B_0}{2} \left( \frac{z+L}{\sqrt{(z+L)^2+r^2}} - \frac{z-L}{\sqrt{(z-L)^2+r^2}} \right) \\
 &\quad - \frac{B_0}{2} \left( \frac{z-L-g}{\sqrt{(z-L-g)^2+R^2}} - \frac{z-3L-g}{\sqrt{(z-3L-g)^2+R^2}} \right) \\
 &\quad + \frac{B_0}{2} \left( \frac{z-L-g}{\sqrt{(z-L-g)^2+r^2}} - \frac{z-3L-g}{\sqrt{(z-3L-g)^2+r^2}} \right),
 \end{aligned}$$

where  $B_0$  is the remanence of the magnetic material and  $g$  is the width of the gap between the two magnets. An equivalent formula for a solitary magnet was given, e.g., in Ref. 4. This can be integrated analytically to give the Faraday rotation angle:

$$\begin{aligned}
 \alpha &= V \int_{z_1}^{z_2} B(z) dz \\
 &= \frac{VB_0}{2} \left( \sqrt{(z_2+L)^2+R^2} - \sqrt{(z_1+L)^2+R^2} \right) \\
 &\quad + \dots \{14 \text{ more terms} \} \dots,
 \end{aligned}$$

where  $z_1$  and  $z_2$  are the positions of the end faces of one of the crystals.

If the magnet length is a few times larger than the bore diameter then the flux density is sufficiently homogeneous



across the diameter of the bore, and the Faraday rotation angle obtained above for a beam exactly on the axis of the magnets is also valid for the whole aperture of the isolator. The effect of fringe fields at the ends of the magnets can be minimized by using crystals that are a few millimeters shorter than the magnets and by centering them in the bore.

The magnets are made from NdFeB. This material has a remanence of up to 1.3 T, a strong magnetic anisotropy, and a high coercivity. This is important because one magnet is operating in the strong demagnetizing field of the other. In our experiments no deviation from linear superposition of the fields of the two magnets was noticeable even at zero separation.

The geometric dimensions of the magnets were chosen such that  $\int B(z)dz$ , taken over the length of one crystal, was 0.011 T m when the magnets were closest together (8 mm). This corresponds to a 45° rotation at  $\lambda=830$  nm. When the magnets are pushed fully apart (28 mm), 45° rotation occurs at  $\lambda=780$  nm. Figure 3 shows the total magnetic flux density along the axis of the isolator. Comparison between the solid and the dashed line shows the increased flux density inside the bore of one magnet due to the presence of the other one.

The angle of rotation was measured for the first crystal of the tandem arrangement and found to be uniform across the full aperture to within our measurement accuracy of 0.5°.

### C. Polarizers

A look at Fig. 2 shows that the overall isolation ratio of the tandem Faraday isolator cannot be better than the amount of light with the “wrong” polarization that is transmitted through the central polarizer, because this light will arrive at polarizer 1 with the “right” polarization to be transmitted. Although this seems to imply that one has to use a crystal polarizer with  $10^{-6}$  extinction to achieve 60-dB isolation we show in the following that a thin-film MacNeille polarizer with an extinction (i.e., transmission through crossed polarizers) of only  $10^{-4}$  is sufficient. Such a polarizer is much more affordable than a crystal polarizer and allows a compact design because it can be small enough to fit in the gap between the two magnets and because it transmits one polarization without change of beam direction while deflecting the other one at 90°.

Thin-film MacNeille-type polarizers<sup>5</sup> consist of a thin-film stack deposited onto the diagonal face of a cemented glass cube (Fig. 4). Light entering through one of the glass prisms GP<sub>1</sub> and GP<sub>2</sub> hits the thin-film stack St at 45°. At the individual stack layers the Brewster condition is fulfilled. This results in high transmission for the *p* wave. *S*-polarized light is partly reflected at each layer. The thickness of the layers is chosen such that constructive interference of the reflected partial waves occurs. With a sufficiently large number of layers the power reflection coefficient for the *s* wave of the entire stack can be made higher than  $1-10^{-7}$ , i.e., less than  $10^{-7}$  of the incident *s*-polarized light passes through the stack. Due to stress-

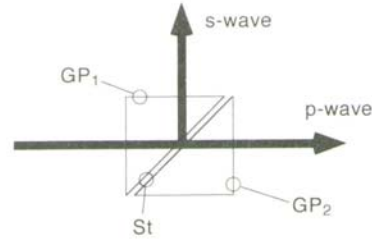


FIG. 4. A thin-film MacNeille polarizer consists of a stack St of dielectric layers sandwiched between two glass prisms GP<sub>1</sub> and GP<sub>2</sub>.

induced birefringence and index inhomogeneities of standard glasses a fraction of  $10^{-4}$ – $10^{-6}$  of the intensity in one polarization mode is coupled into the other mode, thus limiting the extinction.

To determine the limit for the isolation ratio set by the polarizers we first look at one polarizer in detail and derive two equations describing its behavior which we then use to examine the combination of three polarizers in our Faraday isolator. We assume a worst-case scenario here: (i) a transmission of  $10^{-6}$  for the *s*-polarized component at the stack; (ii)  $10^{-4}$  of the power of each component is transformed into the other polarization state by residual birefringence or scattering. We furthermore assume that this effect is nonuniform across the cross section of the beam so that we can do our calculation with intensities instead of electric field amplitudes.

Consider the situation shown in Fig. 4. Unpolarized light with intensities  $s_{in}$  and  $p_{in}$  in the two linear polarization states is transformed by GP<sub>1</sub> into

$$s_{GP_1} = s_{in} + p_{in} \times 10^{-4},$$

$$p_{GP_1} = p_{in} + s_{in} \times 10^{-4}.$$

Behind the stack St we have left

$$s_{St} = s_{GP_1} \times 10^{-6},$$

$$p_{St} = p_{GP_1}.$$

Finally, GP<sub>2</sub> mixes *s* and *p* again:

$$s_{out} = s_{St} + p_{St} \times 10^{-4},$$

$$p_{out} = p_{St} + s_{St} \times 10^{-4}.$$

Putting everything together and keeping only the largest terms we obtain

$$s_{out} = s_{in} \times 10^{-6} + p_{in} \times 10^{-4},$$

$$p_{out} = p_{in} + s_{in} \times 10^{-4}.$$

We can apply these equations to the situation in our Faraday isolator (Fig. 2). Suppose that backscattered light of unit intensity in the *s* and *p* components is incident on polarizer 3 from the right. Behind the polarizer we get

$$s_3 = 10^{-6} + 10^{-4} \approx 10^{-4},$$

$$p_3 = 1 + 10^{-4} \approx 1.$$

The Faraday rotation in crystal 2 and the rotated axis of polarizer 2 lead to an exchange of the roles of  $s$  and  $p$ ; behind polarizer 2 we have

$$s_2 = p_3 \times 10^{-6} + s_3 \times 10^{-4} \approx 10^{-6},$$

$$p_2 = s_3 + p_3 \times 10^{-4} \approx 10^{-4}.$$

The extinction (i.e., the total transmission of the crossed polarizers 2 and 3) is not better than  $10^{-4}$ .

After one more Faraday rotation and transmission through polarizer 1 we obtain

$$s_1 = p_2 \times 10^{-6} + s_2 \times 10^{-4} \approx 10^{-10},$$

$$p_1 = s_2 + p_2 \times 10^{-4} \approx 10^{-6}.$$

The surprising result is that an overall isolation of order  $10^{-6}$  can be achieved with a central polarizer having an extinction of only  $10^{-4}$ .

The polarizers are slightly tilted against the optic axis to avoid direct reflections. The tilting angles were chosen such that the parallel beam displacements of the three polarizers cancel. To reduce transmission losses all surfaces are antireflection coated.

#### IV. TUNING CHARACTERISTICS

Our isolator can be wavelength tuned continuously from 700 to 1000 nm and beyond in two ways. Coarse tuning is achieved by changing the separation of the magnets using a pair of screws; fine tuning employs rotation of the central polarizer with a micrometer drive. The output polarization and the beam position will not change during the tuning process.

##### A. Coarse tuning

The flux density inside the bore of each of the magnets is the sum of the flux densities of both magnets. If the gap between the magnets is increased the total flux density decreases and the angle of rotation gets smaller for a fixed wavelength. But since the Verdet constant increases for shorter wavelengths the Faraday rotation now reaches  $45^\circ$  for a shorter wavelength.

For optimum performance the central polarizer is kept at a fixed angle of  $45^\circ$  with respect to the outer polarizers. The minimum magnet separation of 8 mm was chosen such that the rotation angle is  $\pm 45^\circ$  for  $\lambda = 830$  nm, and at the maximum separation of 28 mm the  $\pm 45^\circ$  rotation occurs at  $\lambda = 780$  nm (Fig. 5). Apart from small dispersion effects in the optical coatings of the various components the insertion loss does not change during tuning.

##### B. Fine tuning

Suppose that, for a certain wavelength and a fixed magnet separation, the rotation angle differs from  $45^\circ$  by  $\Delta\alpha$ . Then the light coming from the reverse direction will see the preferred axis of the central polarizer not at  $90^\circ$  but at  $90^\circ - \Delta\alpha$ . If the polarizer is now rotated by  $\Delta\alpha$  such that its preferred axis makes again a  $90^\circ$  angle with the polarization of the light then the full 60-dB isolation is recovered. The trade-off is that the insertion loss will increase. In

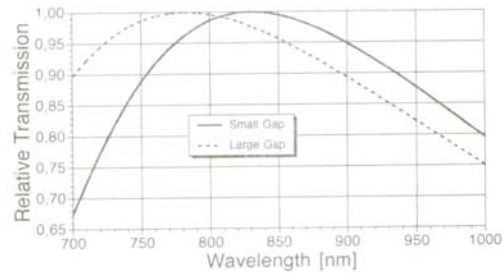


FIG. 5. Tuning curves of the Faraday isolator. The curves show the relative transmission of the whole system when (for fixed magnet separation) the central polarizer's preferred axis is rotated. Solid line: smallest magnet separation; dashed line: largest magnet separation.

the forward direction the central polarizer is rotated by  $2\Delta\alpha$  with respect to the light incident on it so that only a fraction of  $\cos^2(2\Delta\alpha)$  will be transmitted (Malus' law). The same fraction is lost at the output polarizer. In total the insertion loss will increase by a factor of  $1/\cos^4(2\Delta\alpha)$ .

With a micrometer drive the central polarizer can be rotated by approximately  $22^\circ$  in each direction. With that mechanism alone our isolator can be tuned beyond the range from 700 to 1000 nm, but the losses will increase (Fig. 5). Note that in the range from 780–830 nm the tuning can be done by changing only the magnet separation. Since the central polarizer is kept fixed at  $45^\circ$  the insertion loss will remain unchanged at its minimum value.

#### V. RESULTS

The assembled isolator (Fig. 6) has a square base of  $50 \times 50$  mm<sup>2</sup>, a length along the optic axis between 97 and 117 mm (depending on tuning), and a height of 50 mm not including the base and the fine adjustment screw. It weighs

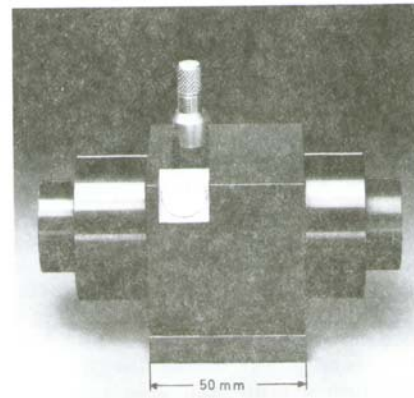


FIG. 6. The assembled Faraday isolator shown in its fully extended position, i.e., tuned to short wavelengths. The cylindrical parts on the right side can be pushed inward to coarse tune the isolator towards longer wavelengths. The micrometer screw is used to fine tune the isolator by rotating the central polarizer. Next to the screw is the antireflection-coated exit window for the beam rejected at the central polarizer.



710 g. Its performance was tested using collimated diode laser modules with emission wavelengths of 789 and 811 nm. The beam cross section was elliptic with an approximate size of  $3 \times 5 \text{ mm}^2$ .

The insertion loss in the forward direction was easily measured using a large-area photodiode (Hamamatsu S2387-1010R precision photometry series). For maximum separation of the magnets we measured a transmission of  $T=89\%$  at  $\lambda=789 \text{ nm}$  when the central polarizer was set for maximum isolation at that wavelength. For minimum separation of the magnets we obtained  $T=88\%$  at  $\lambda=811 \text{ nm}$  when the central polarizer was set for maximum isolation at  $\lambda=811 \text{ nm}$ .

The reverse transmission (i.e., the isolation ratio) could be detected with sensitivity down to  $10^{-7}$  using the same photodiode. The Faraday isolator was placed into the laser beam path in reverse direction. Since no output pattern is detectable at the  $10^{-6}$  level of transmission a reliable alignment procedure of the isolator is essential in order to get correct data.

As a first step, the isolator was positioned using an autocollimation technique such that the housing was exactly perpendicular to the beam. The isolator was then translated keeping its angular orientation unchanged. Since in the reverse direction virtually 100% of the rejected radiation is reflected by the central polarizer at  $90^\circ$  to the laser beam axis, this signal can be used to center the isolator. After that, the alignment could be checked by strongly detuning the central polarizer: this reduced the transmission from more than 60 dB to less than 20 dB, which was enough to recognize any potential cutoff of the transmitted beam profile.

The transmission in the reverse direction was measured for both wavelengths at minimum and maximum separation of the magnets.

Magnet separation	Transmission at $\lambda=789 \text{ nm}$	Transmission at $\lambda=811 \text{ nm}$
minimum	$0.27 \times 10^{-6}$	$0.31 \times 10^{-6}$
maximum	$0.18 \times 10^{-6}$	$0.23 \times 10^{-6}$

All values were well below the design goal of  $10^{-6}$ . We assume that the increased transmission at minimum magnet separation is caused by increased magnetic field inho-

mogeneity across the 5-mm aperture, which is more pronounced for smaller gaps between the magnets.

With the magnets set to minimum separation the isolator could be tuned as far as the  $1.064\text{-}\mu\text{m}$  Nd:YAG line. At this wavelength the reverse transmission was measured to be  $2.5 \times 10^{-6}$ . It must be noted, however, that the insertion loss at this setting is approximately 4 dB.

By changing the mount of the central polarizer to allow for a larger rotation angle it was possible to tune the isolator such that maximum isolation occurred at the visible wavelength of 633 nm. In this setting one could look directly into the (attenuated) laser beam. The beam pattern does not show any circularly symmetric pattern that could be a sign of reduced isolation due to transverse inhomogeneities of the magnetic flux density. The observed irregular brightness distribution instead seemed to indicate that the ultimately achievable isolation ratio is still limited by inhomogeneities in the TGG crystals. This also shows that our assumption made above, that the depolarizing effects are nonuniform over the cross section of the beam, is justified.

Both the flux density of the magnets and the Verdet constant of TGG are temperature dependent. We placed the isolator in a thermally controlled box and checked the overall temperature dependence of the performance. If the central polarizer was set for optimum isolation ratio at a certain temperature the isolation was no worse than 60 dB within a  $\pm 8^\circ\text{C}$  temperature range. To maintain the optimum isolation ratio at all times the central polarizer had to be rotated by  $0.22^\circ$  per Kelvin of temperature change. This translates to 0.05 divisions on the micrometer screw and is usually negligible.

#### ACKNOWLEDGMENT

We thank M. Ledig for many helpful discussions.

<sup>1</sup>L. Rayleigh, *Phil. Trans. Royal Soc. London* **176**, 343 (1885); L. Rayleigh, *Nature* **64**, 577 (1901).

<sup>2</sup>K. P. Birch, *Opt. Commun.* **43**, 79 (1982).

<sup>3</sup>U. V. Valiev, G. S. Krinchik, S. B. Kruglyashov, R. Z. Levitin, K. M. Mukimov, V. N. Orlov, and B. Yu. Sokolov, *Sov. Phys. Solid State* **24**, 1596 (1982).

<sup>4</sup>K. Shiraishi, F. Tajima, and S. Kawakami, *Opt. Lett.* **11**, 82 (1986).

<sup>5</sup>S. M. MacNeille, U. S. patent 2 403 731 (July 9, 1946); M. Banning, *J. Opt. Soc. Am.* **37**, 792 (1947).